International Journal of Computational Intelligence in Control
Vol. 13 No. 1 (June, 2021)

System Identification and Intelligent Servo Tuning for Linear Motor on CNC Machine

Chih-Cheng Peng [a], Cheng-Hsin Hsu [b], and Thong-Shing Hwang [b] *

[a] *Graduate Institute of Electrical and Communications Engineering, Feng Chia University, 40724, Taiwan, R.O.C.*

[b] *Graduate Institute of Automatic Control Engineering, Feng Chia University, 100, Wenhwa Road, Seatwen, Taichung 40724, Taiwan, R.O.C.*

*E-mail: tshwang@fcu.edu.tw

Received : 19th September 2020 **Revised on 23rd October 2020;** **Accepted: 16th November 2020**

ABSTRACT

This research presents a system identification method for a linear motor-based 5-axis CNC machine and establish a servo tuning mechanism for Fuzzy-PID control gains. For linear motor identification, an identification method is developed using the inverse discrete Fourier transform (DFT) and balanced realization. For intelligent tuning of the servo system, the fuzzy inference mechanism adjusts servo control gains in a real-time manner which drives the dynamic response to track a desired behavior output. This makes it able to against the load changes while ensuring manufacturing accuracy. Our proposed design is to be realized via an RTLinux based multi-task data acquisition system and TCP/IP network transmission protocol for intelligent tuning of the servo system.

Keyword: System Identification, linear motor, servo tuning, Fuzzy-PID control.

1. Introduction

Due to motor-based 5-axis CNC's mechanism and process are complex, therefore, it is important to use some of intelligent features to help users of the client besides the high rigidity of machine structure and stability design of hot errors, such as rotating axis error correction-compensation, intelligent servo machine tuning and collision monitoring technologies, so that it can ensure processing efficiency, accuracy and reliability. In addition, the properties of the exact accuracy and fast response for linear motor have gradually led to high attention of tool-machining industry recently. For example, national GENTEC [2, 5] has already applied the linear motor to the wire slicing of the accurate molding process. While German DMG corporate utilizes linear motor on 5-axis process machine of high speed and high accuracy, its applications include accurate machine parts, medical equipment, and accurate molds, etc.

The bigger air-gap and lower efficiency problems exist with linear motor in the past. Although linear motor's appearance was almost the same time as traditional rotating motor, the developing progress was in a big lag. However, there are many industry places require high speed and linear-moving. Traditional rotating motor has to achieve the goal through gears, lead ball screws, and straps. But these kinds of motors have some problems that are low transmission efficiency, complex structure, nonlinear, high noise and low speed, etc. All the problems are the urgent problems of the semiconductor manufacturing and tool-machining industries which need to be solved in order to raise productivity. For example, the traditional electrical discharge machining (EDM) machine's Z-axis actuators are used to arrange ball screw and linear-slide. And the speed of screw's moving is 2m/min~5m/min in general. But when using ball screw, the transmission mechanism such as screw and couplings would lead to the lag of achieving actual position and affect the accuracy and speed of servo. Compared to these disadvantages, linear servo-motor's greatest advantages are high speed displacement, big propulsion, and highly accurate positioning. Moreover, the highly stability and highly prolong the life of equipment, especially for high speed transport and processing tool-machining. And because these advantages, there are some CNC manufacture industry starting to develop linear-motor as the basic CNC equipment [3, 4].

In order to achieve the effects of excellent motor positioning, rotational speed control and good robust performance while load-changing or signal-coupling happens which will lead to accuracy degradation problem. As for how to execute dynamic mode identification and high efficiency servo tuning on CNC driving motor through internet in real-time, it is the main purpose of this research. So, this article introduces some methodologies to carry out dynamic mode identification and intelligent tuning technique through RTLinux hard-real-time multi-task system and TCP/IP instant network transport mechanism. That means the purpose of this article is to establish a set of 5-axis CNC intelligent internet instant servo tuning technique system.

This research is to develop the necessary CNC software kernel and additive valuable software technique of the domestic linear-motor 5-axis tool-machining by using the well-developed CNC controller of project coordinate Co. Ltd. —GENTEC.

2. System Architecture

The purpose of this research is to set up an RTLinux hard-real-time [9] multi-task executive system, TCP / IP network transport mechanism instantly and a 5-axis CNC network instant servo tuning system. System architecture is shown in Fig.1.

3. System Identification

Because the linear motor is actually a nonlinear system, it is more difficult to establish the real dynamic model. Here, we use the experimental identification method to find the linear motor model under the consideration of different loading change. During the experiment, assuming the system dynamic behavior to be operated near the operation-point with minor variation, therefore small change of the dynamic behavior can be regarded as a linear time-invariant system, and then we can get the dynamic model of the linear motor. In this research, first, we adopt Panasonic PANA TERM software provided by company GENTEC to identify the model of linear motor, and execute this task on the company's linear motor machine, as shown in Fig. 1. Figure 2 is the PANA TERM software operating scenarios. Secondary, we use inverse discrete Fourier transform (IDFT) [1] and balancing realization technique to accomplish the same system identification task.

3.1 System Identification Using PANA TERM

PANA TERM software is used to perform system identification of the single-axis linear motor machine. The resulting frequency response of the Bode diagram is shown in Fig.3 and Fig.4. In Fig.3, the Bode Diagram of system identification is got by using the mover weight 4.5 kg for the linear motor, and Fig.4 is for the 9 kg mover.

With the above Bode Diagram we can derive the transfer function of the linear motor dynamic model as follows：

(a) For linear motor mover 4.5 kg, the dynamic transfer function can be obtained as follows and its frequency response Bode Diagram is shown in Fig.5.

$$G(s)=\frac{(1+\frac{s}{200})}{(1+\frac{s}{150})(1+\frac{2s}{250}+\frac{s^2}{(250)^2})}$$

(b) For linear motor mover 9 kg, the dynamic transfer function can be obtained as follows and its frequency response Bode Diagram is shown in Fig.6.

$$G(s)=\frac{(1+\frac{s}{200})}{(1+\frac{s}{120})(1+\frac{2s}{230}+\frac{s^2}{(230)^2})}$$

3.2 System Identification Using Balancing Realization

Dynamic model identification of the linear motor system is necessary for the design of auto-tuning Fuzzy-PID [6,-8, 12] controller. In this paper, we use the inverse discrete Fourier transform (IDFT) and balancing realization (BR) synthesis method to accomplish the system identification for a linear motor dynamic model [10, 11]. The practical system identification method includes: (a) input a sinusoidal signal at different frequencies, (b) measuring the output signal to compute the magnitude and phase of the system transfer function, (c) using the Bode plot result to perform the inverse discrete Fourier transform and (d) synthesizing the impulse response to the final transfer function using the balancing realization method. The detailed procedure is listed as follows:

(1) Tustin transform (bilinear transform)

The Bode plot is a curve diagram of the system gain and phase versus frequency, so it is the frequency response plot of the system transfer function. Therefore, in this paper we adopt the IDFT transform which samples the N point in z-domain unit circle. The corresponding angle θ_k equals to $2\pi k/N$, where $k=0,\ 1,\ldots,\ N-1$, so we must determine the corresponding angular frequency (ω) in the s-domain. The method is described below.

$$s=\frac{2}{T}\frac{z-1}{z+1}=j\omega_k=\frac{2}{T}\frac{e^{j\theta_k}-1}{e^{j\theta_k}+1}=\frac{2}{T}\frac{j\sin\theta_k}{1+\cos\theta_k}$$

hence

$$\omega_k=\frac{2}{T}\frac{\sin\theta_k}{1+\cos\theta_k} \tag{1}$$

where T is the sampling period, θ_k equals to $2\pi k/N$. After the sampling period is chosen, we can set up a contrast table between the θ_k and ω_k , where $k=0,\ 1,\ldots,\ N-1$.

(2) Obtain the discrete system response $P\left(e^{j(2\pi/N)k}\right)$ from Bode plot

Assume a system transfer function be $P(s)$, then the discrete system transfer function is

$P(z) = P(s) \quad | \quad s = \frac{2}{T}\frac{z-1}{z+1}$, namely $P(e^{j\theta_k}) = P(j\omega_k)$. Therefore, $P\left(e^{j(2\pi/N)k}\right)$ can be obtained from the Bode plot magnitude and phase of the corresponding N point frequency.

(3) Computation impulse response $h(i)$ via IDFT

To begin with, we will express the formula of IDFT below.

$$h(n) = \frac{1}{N}\sum_{n=0}^{N-1} P(e^{j\frac{2\pi k}{N}})e^{j\frac{2\pi kn}{N}} \tag{2}$$

(4) Synthesize the system transfer function through $h(i)$ and BR method

Consider a system transfer function

$$P(s) = \frac{\beta_1 s^{n-1} + \beta_2 s^{n-2} + \ldots\ldots + \beta_{n-1}s + \beta_n}{s^n + \alpha_1 s^{n-1} + \alpha_2 s^{n-2} + \ldots\ldots + \alpha_{n-1}s + \alpha_n} \tag{3}$$

Expanding Equation (3) as a power series yields:

$$P(s) = h(0) + h(1)s^{-1} + h(2)s^{-2} + \ldots\ldots \tag{4}$$

We can obtain the Hankel matrix $T(\alpha, \beta)$:

$$T(\alpha,\beta) = \begin{bmatrix} h(1) & h(2) & h(3) & \cdots & h(\beta) \\ h(2) & h(3) & h(4) & \cdots & h(\beta+1) \\ h(3) & h(4) & h(5) & \cdots & h(\beta+2) \\ \vdots & \vdots & \vdots & \ddots & \vdots \\ h(\alpha) & h(\alpha+1) & h(\alpha+2) & \cdots & h(\alpha+\beta-1) \end{bmatrix} \tag{5}$$

If (A, b, c) is the realization of $P(s)$, then

$$\begin{aligned} P(s) &= c(sI - A)^{-1}b \\ &= h(1)s^{-1} + h(2)s^{-2} + h(3)s^{-3} + \ldots\ldots \end{aligned} \tag{6}$$

if only and if $h(m) = cA^{m-1}b$, $m = 1,2\ldots\ldots$, then (A, b, c) is the realization of $P(s)$. Substituting $h(m) = cA^{m-1}b$ into Hankel matrix $T(n, n)$, we can get

$$
T(n,n)=\begin{bmatrix} cb & cAb & cA^2b & \cdots & cA^{n-1}b \\ cAb & cA^2b & cA^3b & \cdots & cA^nb \\ cA^2b & cA^3b & cA^4b & \cdots & cA^{n+1}b \\ \vdots & \vdots & \vdots & \ddots & \vdots \\ cA^{n-1}b & cA^nb & cA^{n+1}b & \cdots & cA^{2(n-1)}b \end{bmatrix}
= \begin{bmatrix} c \\ cA \\ \vdots \\ \vdots \\ cA^{n-1} \end{bmatrix} \begin{bmatrix} b & Ab & \cdots & \cdots & A^{n-1}b \end{bmatrix} = OC \tag{7}
$$

where O is the observability matrix, C is the controllability matrix. Define

$$
\tilde{T}(n,n)=\begin{bmatrix} h(2) & h(3) & h(4) & \cdots & h(n+1) \\ h(3) & h(4) & h(5) & \cdots & h(n+2) \\ h(4) & h(5) & h(6) & \cdots & h(n+3) \\ \vdots & \vdots & \vdots & \ddots & \vdots \\ h(n+1) & h(n+2) & h(n+3) & \cdots & h(2n) \end{bmatrix}
= \begin{bmatrix} c \\ cA \\ \vdots \\ \vdots \\ cA^{n-1} \end{bmatrix} A \begin{bmatrix} b & Ab & \cdots & \cdots & A^{n-1}b \end{bmatrix} = OAC \tag{8}
$$

If the system is controllable and observable, then the controllable Gramian W_c and the observability Gramian W_o are positive definite. (W_c, W_o) is a unique solution of the following equation:

$$
AW_c + W_cA' = -bb' \quad , \quad A'W_o + W_oA = -c'c \tag{9}
$$

where A' is the transpose of A. For a transfer function, different minimal realization has different W_c and W_o, but the product of W_c and W_o is still same.

Because W_c is a symmetric matrix of real number, it exists an orthogonal matrix Q such that $W_c = Q'DQ$. Where D is a diagonal matrix including the eigenvalue of W_c. At the same time, we can also compute to get

$$
W_c = Q'DQ = Q'D^{1/2}D^{1/2}Q = R'R \tag{10}
$$

and

$$W_c W_o = R'RW_o = RW_oR' = U\sum{}^2 U' \tag{11}$$

where $\Sigma = diag(\sigma_1, \sigma_2, \ldots\ldots, \sigma_n)$, σ_i is a singular value, and U is an orthogonal matrix (i.e. $U'U = I$).

Given that an existing similarity transformation $\bar{x} = px$, and

$$p = \sum{}^{1/2} U'(R')^{-1} \quad , p' = R^{-1} U \sum{}^{1/2}$$

$$p^{-1} = R'U \sum{}^{-1/2} \quad , p'^{-1} = \sum{}^{-1/2} U'R \tag{12}$$

then

$$\bar{W}_c = PW_cP' = \sum{}^{1/2} U'(R')^{-1} W_c R^{-1} U \sum{}^{1/2}$$

$$= \sum{}^{1/2} U'(R')^{-1} R'RR^{-1} U \sum{}^{1/2} = \sum$$

$$\bar{W}_o = P'^{-1} W_o P^{-1} = \sum{}^{-1/2} U'RW_oR'U \sum{}^{-1/2}$$

$$= \sum{}^{-1/2} U'U \sum{}^2 U'U \sum{}^{-1/2}$$

$$= \sum{}^{-1/2} \sum{}^2 \sum{}^{-1/2} = \sum \tag{12}$$

Therefore, we can say that if the controllability Gramian W_c and observability Gramian W_o for the equation of possessing minimal equivalent state value have the property of $\bar{W}_c = \bar{W}_o = \Sigma$, this realization is namely a minimal balancing realization.

So if we can obtain the Hankel matrix $T(n, n)$ through the IDFT transform, utilizing singular value decomposition (SVD) again, then we can compute to obtain

$$T(n,n) = K\sum L' = K\sum{}^{1/2} \sum{}^{1/2} L' = OC \tag{13}$$

where both K and L are the orthogonal matrices, so we can obtain

$$O^{-1} = \sum{}^{-1/2} K' \quad , C^{-1} = L\sum{}^{-1/2} \tag{14}$$

where K' is the transpose of the conjugate complex of matrix K. From $\tilde{T}(n,n) = OAC$, we can get

$$A = O^{-1} \tilde{T}(n,n) C^{-1} \tag{15}$$

and b equals the first column of C and c equals the first row of O. Finally, the transfer function $P(z)$ can be synthesized via (A, b, c), namely:

$$P(z) = c(zI - A)^{-1} b \tag{16}$$

Again through $s = \frac{2}{T}\frac{z-1}{z+1}$ Tustin transform, the $P(z)$ can be transformed into $P(s)$.

(5) Dynamic model identification of linear motor

The experimental steps for parameter identification of the linear motor dynamic model are as follows:

(a) Obtain the angular speed ω in the experimentation：

We sample 256 points within the unit circle of the z-domain and the corresponding angle is $\theta_k = 2\pi k/256$, and $k = 0, 1,\ldots, 255$, $T = 0.1$ sec., thus getting the angular speed in s-domain below：

$$s = \frac{2}{T}\frac{j\sin\theta}{1+\cos\theta} \Rightarrow \omega_k = 20\frac{\sin\theta_k}{1+\cos\theta_k},\ \theta_k = \frac{2\pi k}{256} \tag{17}$$

(b) Calculate the magnitude and phase

In the experimentation, let the linear motor mover perform the go-and-back motion via a sine wave with the amplitude of 50 mm. Record the input position command for mover and measure the mover real position values from photometer. We take a stable wave period to calculate the magnitude and phase, gain and phase can be considered as follows in Fig. 7.

(c)Transfer function synthesis

We put 256 sets values into the ifft function of MATLAB package software, the acquired $h(m)$ (Hankel parameters) values will be put into the SVD (Singular Value Decomposition) function of MATLAB again to obtain the coefficients of the numerator and denominator in the transfer function. So we can get the transfer function of $P(z)$, transform $P(z)$ into $P(s)$ again. Adding $h(0)$ into the transfer function $P(s)$, which was not includes previously, and the overall transfer function can be obtained as

$$P(s) = \frac{0.07227s^3 + 28.58s^2 + 11349.71s + 3183.515}{0.1173s^3 + 73.69s^2 + 1502.04s + 3544.8}$$

The Bode plot for the synthetic transfer function is shown in Fig. 8.

4. Dynamic Tracking

Because the input sin-wave signal of different frequency and measured output signal are processed by PC for the practical system identification method. Therefore, this kind of identification method for the dynamic model is able to identify online in real-time. Moreover, in this research, we use Fuzzy-PID dynamic output synchronous tracking for the intelligent real-time servo tuning. It is simple and actual to adjust PID gain quickly under the changing of practical loading, and it can make the linear motor's dynamic output response to approach the desired dynamic output response of the performance index.

Therefore, if the single-axis linear motor of the hardwire-in-the-loop has to achieve the real-time servo tuning purpose, it must adopt dynamic synchronous tracking methodology, as shown in Fig. 9. Here, we add a Fuzzy inference to adjust k_p, k_i, k_d of PID controller in the linear motor hardwire-in-the-loop system so that the linear motor dynamic output response can approach the desired dynamic output response of the transfer function got from system identification. By using the simple tracking method the system could increase the adaptability, robustly and sensitivity so that it can compensate the changing or uncertainty of controlled model and machine. Mathematical model is the leading linear motor dynamic model, and hardwire-in-the-loop linear motor is the following actual linear motor system (using a little different dynamic model while tracking simulation), e_1 is the error of two dynamic output responses, $\dot{e}_1$ is the changing rate of e_1, and e_2 is the error in hardwire linear motor feedback loop. In the adaptation of single-axis linear motor real-time servo tuning, if loading (the normal force of linear motor mover) produces changing, and then adopt the performance tracking mechanism to run real-time tuning task.

In order to make the following linear motor can keep up with leading dynamic model output response, we add Fuzzy inference to speed up the convergence. By converting Fuzzy inference expert knowledge or experiment control strategy into automatic Fuzzy rule, and classifying the input data, consulting the Fuzzy rule, as shown in Table 1, to produce corresponding Fuzzy output. Finally, defuzzification process is applied to produce output. Figure 10 is the SIMULINK block diagram of auto-tuning mechanism, and the detailed block diagram of Fuzzy controller is shown in Fig. 11. Figure 12 illustrates the simulation results for the proposed Fuzzy-PID control design and without loading of the single-axis linear motor system of GENTEC. Figure 12 shows that the Fuzzy-PID controller can improve the stability and transition response of the system.

5. Conclusion

As the above description, this research uses Fuzzy inference to adjust k_p, k_i, k_d of PID controller in the linear motor hardwire-in-the-loop system so that the linear motor dynamic output response can approach the desired dynamic output response of the transfer function got from system identification. By using the simple tracking method the system could increase the adaptability, robustly and sensitivity so that it can compensate the changing or uncertainty of controlled model and machine.

The final goal of this research is to develop an intelligent servo tuning technique equipment and apply this technique to the practical 5-axis CNC tool-machining on accurate machine element, accurate mold, and medical equipment. Now, this research has accomplished a set of linear motor system identification and real-time servo tuning. Through numerical and experimental verification, the demonstration shows that the method is feasible and the dynamic synchronous tracking, system identification online, and servo auto-tuning will be realized on 5-axis CNC machine in the future.

Acknowledgement

This research was sponsored by National Science Council, Taiwan, R.O.C. under the grant NSC 102-2218-E-005-012.

References

[1] T. S. Hwang, S. W. Chen, K. H. Chan, and J. C. Tsai, “Intelligent two-axis dual-CCD image-servo shooting platform design,” *Int. J. Research on Eng. and Tech.*, Vol. 3, pp. 329-334, 2014.

[2] S. P. Hsieh, and T. S. Hwang, “Dynamic modeling and neural network self-tuning PID control design for a linear motor driving platform,” *IEEJ Trans.*, Vol. 5, pp. 701-707, 2010.

[3] Y. J. Lin, T. S. Hwang, C. C. Peng, C. Y. Chang, and W. R. Lai, “Neural network path-tracking and real-time multi-task flight simulation for the automatic transition of tilt-rotor aircraft,” *Proc. Asian Control Conf.*, Kaohsiung, pp. 459-464, 2011.

[4] C. C. Peng, T. S. Hwang, C. Y. Chang, Y. T. Wu, and S. H. Wu, “Real-time simulation of a 3-leg 6-DOF parallel manipulator based on RT-Linux operation system,” *Proc. IEEE Int. Conf. Robotics*, Automation and Mechatronics, pp. 297-302, 2010.

[5] K. Erkorkmaz, Y. Altintas, and C.-H. Yeung “Virtual computer numerical control system,” *CIRP Annals - Manufacturing Tech.*,Volume 55, Issue 1, pp. 399-402, 2006.

[6] M. Cheng, Q. Sun, and E. Zhou, “New self-tuning Fuzzy PI control of a novel doubly salient permanent-magnet motor drive”, *IEEE Trans. Industrial*

Electronics, Vol.53, pp. 814-821, 2006.

[7] W. C. Wang, and C. H. Lee, "Fuzzy neural network-based adaptive impedance force control design of robot manipulator under unknown environment," *IEEE Int. Conf. Fuzzy Syst.*, pp. 1442-1448, 2014.

[8] D. Rached, A. Yousef, and H. Wissam, "A self tuning PID controller using wavelet networks," *IEEE Int. Conf. Power Electronics Specialists*, pp. 773-777, 2008.

[9] C. H. Tang, "Identification of dynamic system and real time simulation for high speed linear motor driving platform" , Master Thesis, Graduate School of Mechanical and Aerospace Engineering, Chung Hua University, Hsinchu, Taiwan, 2000.

[10] K. Fujimoto and D. Tsubakino, "Nonlinear balanced realization based on singular value analysis of Hankel operators," in *Proc. 42nd IEEE Conf. on Decision and Contro*l, pp. 6072-6077, 2003.

[11] K. Fujimoto, and D. Tsubakino, "On computation of nonlinear balanced realization and model reduction," in *Proc. American Control Conf.*, pp. 460-465, 2006.

[12] F. J. Lin, and P. H. Chou, "Adaptive control of two-axis motion control system using interval type-2 fuzzy neural network," *IEEE Trans. Industrial Electronics*, Vol.5, pp. 178-193, 2009.

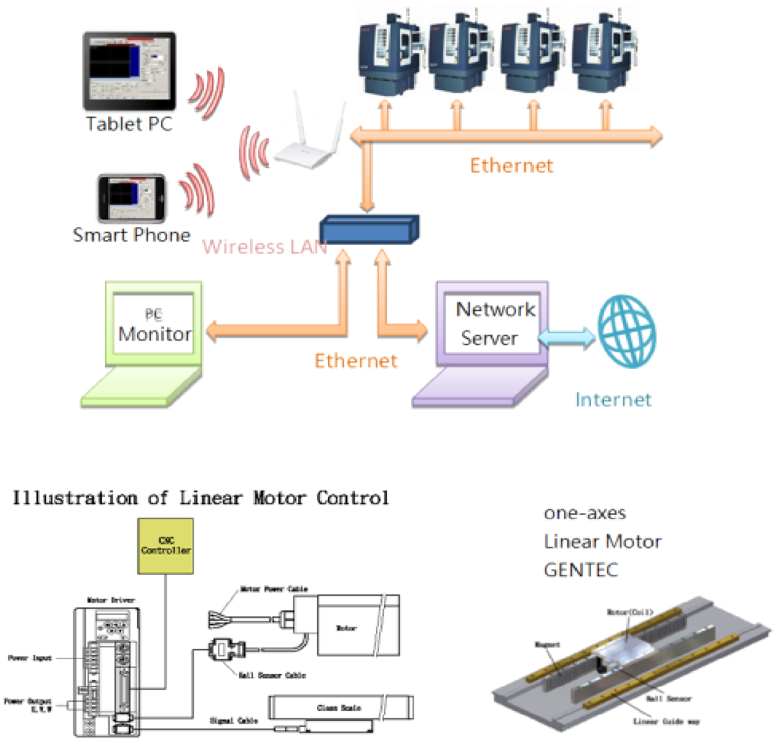

Fig. 1 System architecture of the network monitoring servo tuning system and linear-motor machine

Fig. 2 PANA TERM software operating scene

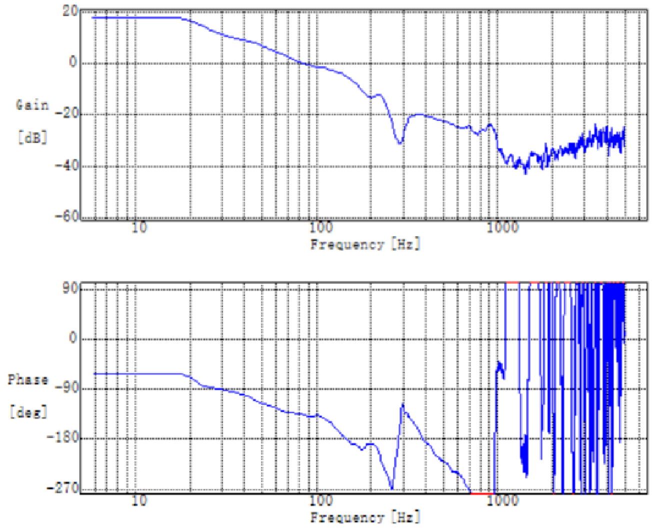

Fig. 3 Bode diagram of linear motor system for the mover mass of 4.5 kg

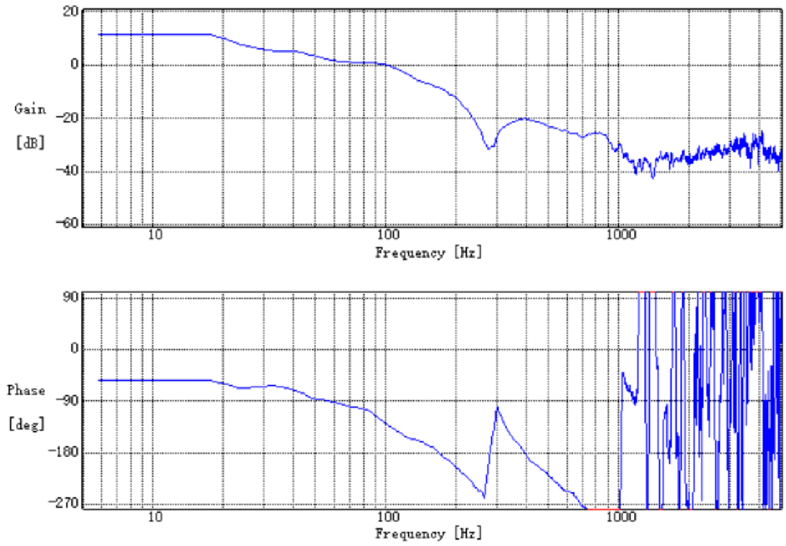

Fig. 4 Bode diagram of linear motor system for the mover mass of 9 kg

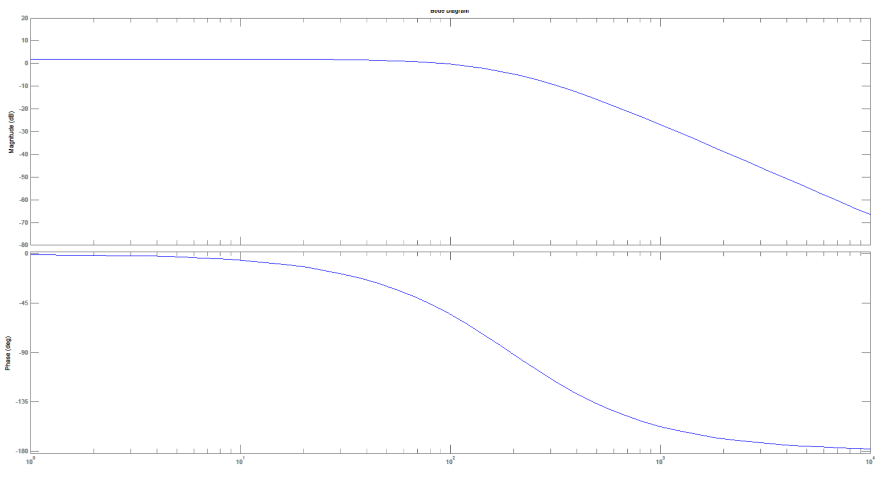

Fig. 5 Bode diagram of linear motor transfer function for mover mass of 4.5 kg, Frequency (angular velocity, ω)

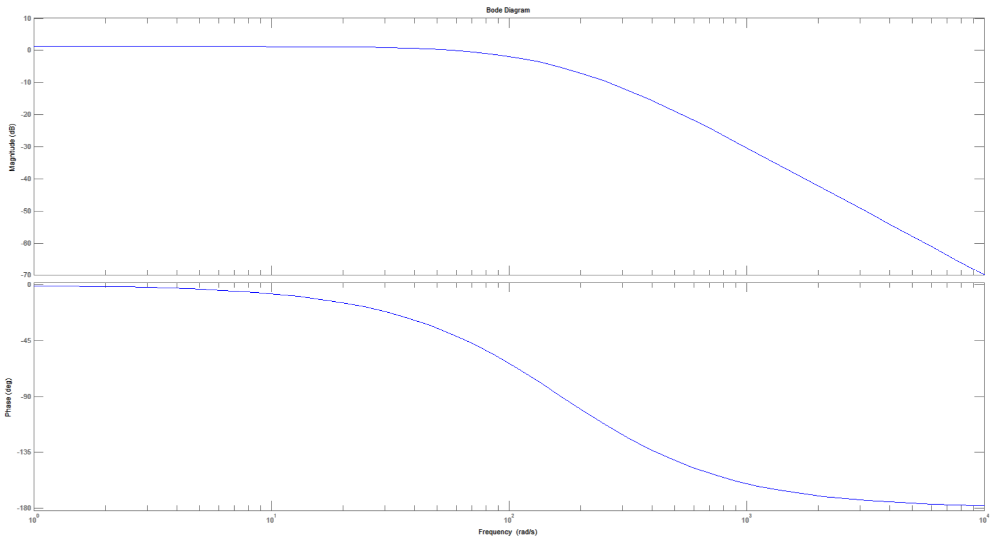

Fig. 6 Bode Diagram of linear motor transfer function for mover mass of 9 kg, Frequency (angular velocity, ω)

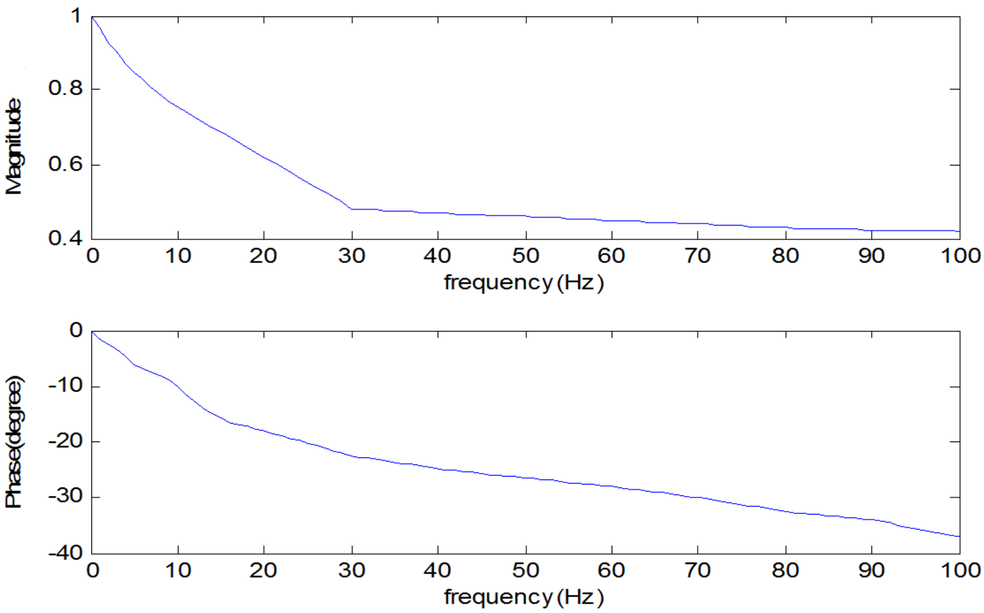

Fig. 7 Bode plot for system transfer function via experimental results

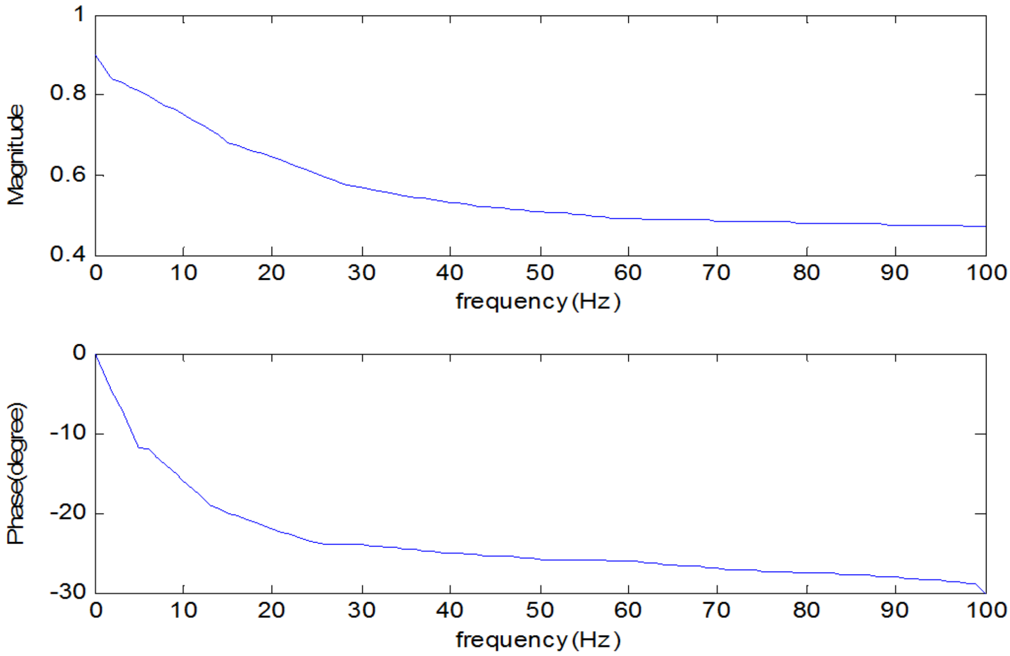

Fig. 8 Bode plot for synthetic transfer function

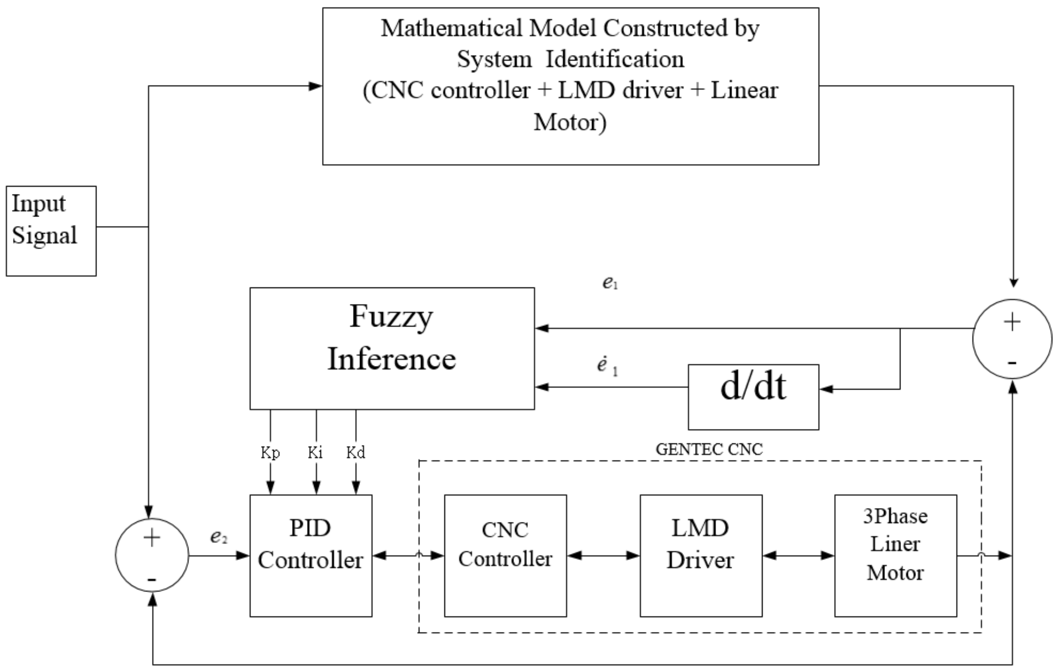

Fig. 9 Intelligent Servo Tuning for Linear Motor on CNC Machine

Table 1. Fuzzy rule

e_1 \ $\dot{e}_1$	NB	NM	NS	ZO	PS	PM	PB
NB	PB/NS/PS	PB/ZO/PS	PM/NB/ZO	PS/NM/ZO	PS/NM/ZO	PS/ZO/PM	ZO/PS/PB
NM	PB/NS/NM	PB/ZO/NS	PM/NM/NS	PS/NS/ZO	PS/NS/ZO	ZO/ZO/PM	ZO/PS/PM
NS	PM/NS/NB	PM/ZONB	PMNS/NM	PS/ZO/NS	ZO/ZO/ZO	NS/PS/PS	NS/PS/PM
ZO	PM/NS/NB	PM/ZO/NM	PS/NS/NM	ZO/ZO/NS	NS/PS/ZO	NM/PS/PS	NM/PM/PM
PS	PS/NS/NM	PS/NS/NM	ZO/ZO/NS	NS/PS/ZO	NS/PS/ZO	NM/PM/PS	NM/PM/PS
PM	PS/NS/NM	ZO/ZO/NS	NS/PS/NS	NM/PM/NS	NM/PM/ZO	NM/ZO/PS	NB/PS/PS
PB	ZO/NS/PS	NS/ZO/PS	NS/PS/ZO	NM/PM/ZO	NM/PB/ZO	NB/ZO/PB	NB/PS/PB

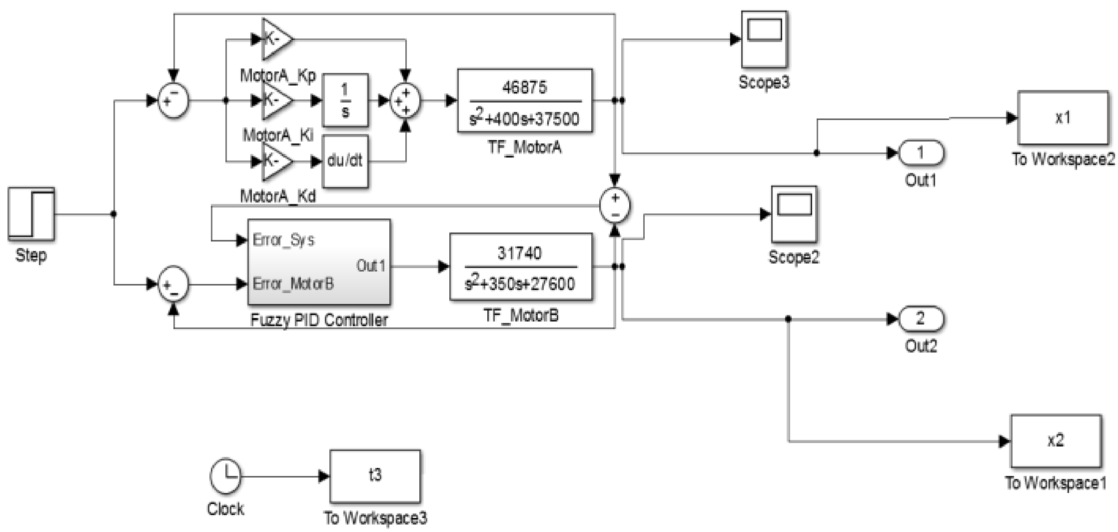

Fig. 10 Block diagram of auto-tuning mechanism with Fuzzy-PID Controller

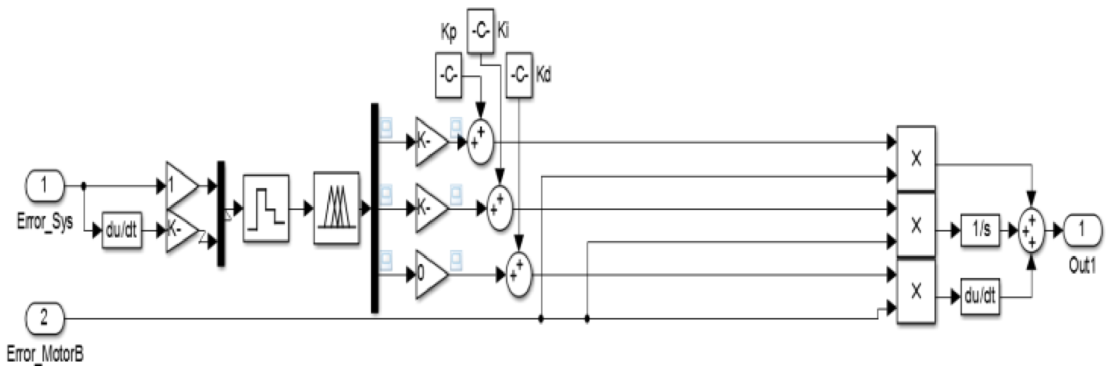

Fig.11 Detailed block diagram of Fuzzy Controller

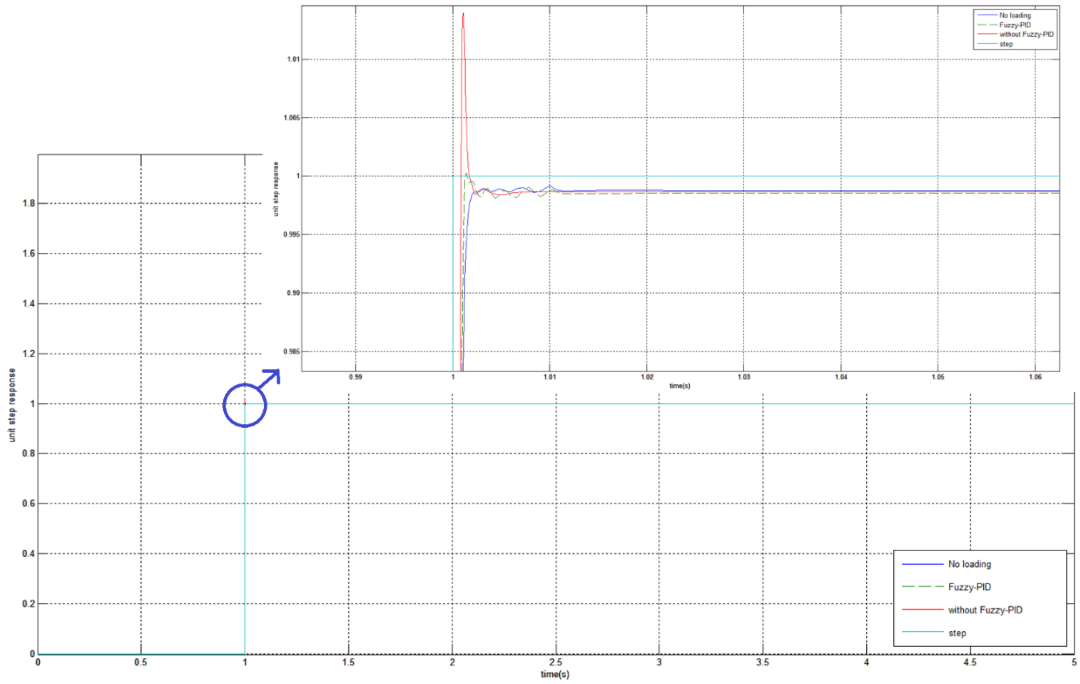

Fig.12 Dynamic response comparisons of without Fuzzy-PID and Fuzzy-PID auto-tuning simulation